Int. J. Electrochem. Sci., 3 **(2008)** 1268 - 1276

International Journal of ELECTROCHEMICAL SCIENCE
www.electrochemsci.org

Large-Scale Synthesis of Monodispersed Carbon Microflakes for Electric Double-Layer Capacitors

Dingsheng Yuan[*], *Jingxing Chen, Xiangchun Hu, Jianghua Zeng, Sanxiang Tan, Yingliang Liu*

Department of Chemistry, Jinan University, Guangzhou 510632, China
[*]E-mail: tydsh@jnu.edu.cn

Received: 20 August 2008 / *Accepted:* 31 August 2008 / *Published:* 4 October 2008

A carbon microflake has been prepared using phenolic resin and acetate magnesium as carbon source by one-step pyrolysis method and then activated with molten KOH at 600°C for 1h in nitrogen atmosphere. As-synthesized products have been characterized by scanning electron microscopy, X-ray diffraction, Raman spectroscopy, N_2 adsorption-desorption and electrochemical measurement. The characterization results indicate that carbon microflakes after the activation possess microporous structure and relatively larger specific surface area (632 m^2 g^{-1}). Raman spectra reveal the defect on its surface is increased. The gravimetric specific capacitance (186.5 F g^{-1}) of the activated carbon microflakes is significantly improved. The high area-normalized specific capacitance (30 μF cm^{-2}) is obtained.

Keywords: Carbon microflakes; Activation; specific surface area; Specific capacitance

1. INTRODUCTION

In recent years, novel carbon materials have attracted considerable attention because of their novel morphologies and specially physical and chemical properties, such as carbon micro-trees [1], mesoporous carbon [2], carbon nanohorns [3], coin-like carbon materials [4], carbon spheres [5], and so on. Carbon nanoflakes as a byproduct of synthesized carbon nanotubes were firstly reported by Ebbesen and Ajayan in 1992 [6]. Carbon nanoflakes have been prepared by novel synthesis methods for their application in past several years [7~9]. However, no literature has been reported on carbon nanoflakes as electrode materials for supercapacitors.

The phenolic resin as a suitable carbon precursor for the preparation of carbon materials has been successfully employed to fabricate novel carbon, such as spherical carbon [10, 11], carbon

membranes [12~14] and ordered arrangement of carbon nanotubes [15]. To the best of our knowledge, there are not the facile methods to directly synthesize the large-scale monodispersed carbon nanoflakes. Therefore, a simple and applied synthesis route should be discovered.

In this work, we have been directly synthesized the carbon microflakes with phenolic resin and acetate magnesium by one-step pyrolysis route. As-prepared carbon microflakes have been activated with molten KOH. The electrochemical capacitive properties for this material have been characterized via cyclic voltammetry and galvanostatic charge/discharge experiments. The results show that the activated carbon microflakes exhibit good electrochemical performance.

2. EXPERIMENTAL PART

2.1. Synthesis of activated carbon microflakes

The mixture of phenolic resins and magnesium acetate were added to a stainless steel autoclave and heated to 600°C at a heating rate of 10°C min^{-1} and maintained at 600°C for 15 h, 20 h and 25 h, respectively, and then cooled to room temperature naturally. The sample was treated with diluted hydrochloric acid and washed by distilled water and dried at 60°C in vacuum for 6 h. The as-synthesized carbon microflakes were referred as CMFs. CMFs prepared for 25 h were uniformly mixed with KOH solid at mass ratio of 1:4. Subsequently, the CMFs were activated at 600°C for 1h in nitrogen atmosphere and denoted as ACMFs.

2.2. Characterization of carbon materials

The X-ray diffraction (XRD) patterns were recorded on a MSAL-XD2 diffractometer using Cu *K*α radiation (36 kV and 20mA, λ□0.154056 nm). Scanning electron microscopy (SEM) images were taken on a Philips XL-30S using an accelerating voltage of 20 kV. Nitrogen adsorption-desorption measurements were performed using a Micromeritics Tristar 3000 system. Raman spectrum was recorded at the ambient temperature on a Renishaw RM2000 Raman micro-spectrometer with an argon-ion at an excitation wavelength of 514.5 nm.

2.3. Electrochemical Performance

A working electrode was fabricated as follows: A foam nickel (10×20 mm) substrate was covered by the mixtures of carbon materials and PTFE (19:1 wt%) and dried at 65°C and then pressed at 25 MPa for 10min. All electrochemical measurements were performed in a three-electrode cell containing NiOOH as an auxiliary electrode and Hg-HgO as a reference electrode. Cyclic voltammograms and galvanostatic charge/discharge curves for the electrodes were measured in the electrolyte 6 mol L^{-1} KOH aqueous solution by a CHI 660B electrochemical workstation.

3. RESULTS AND DISCUSSION

Reaction time is critical for the preparation of carbon microflakes. CMFs prepared for different time are shown in Fig. 1. According to the observation of SEM, monodispersed carbon flakes are successfully prepared from phenolic resin and magnesium acetate via a high temperature thermal decomposition for 15□25 h. Fig. 1d indicates that the thickness of flakes is 190 nm. For comparison, the contrastive experiments were carried out for investigating the influence of magnesium acetate. With phenolic resin or magnesium acetate as precursor, glassy carbon or carbon nanotubes [16] is obtained, respectively. Though we do not clearly understand an effect on magnesium acetate, magnesium acetate kept an important role in the preparation of CMFs.

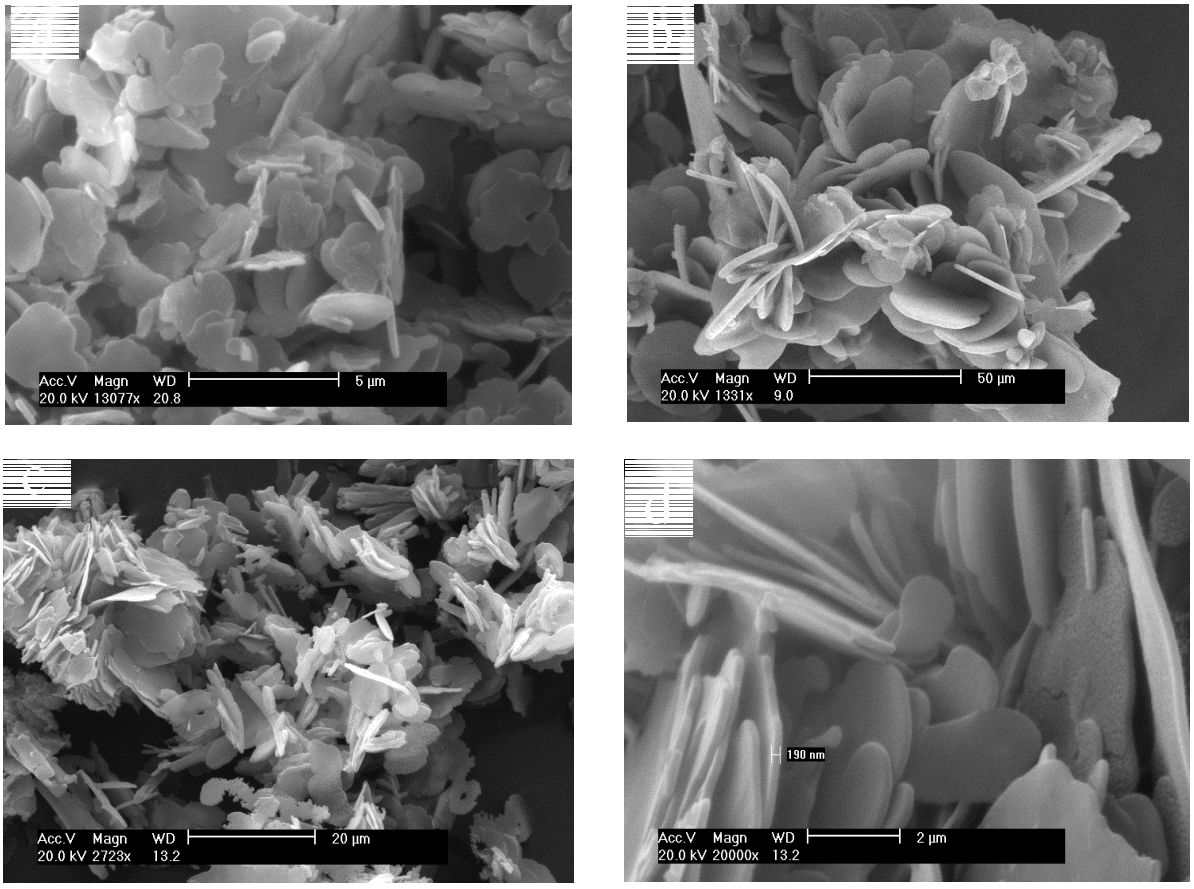

Figure 1. SEM images of carbon microflakes prepared for different time. a□15h□b□20h□c□25h; d: high-magnification image of Fig.1 c.

XRD is applied to analyze the structure of CMFs and ACMFs. Fig. 2a presents the XRD patterns of the samples before and after the treatment by dilute HCl. According to the index JCPDS File No. 08-0479 and 75-1621, as-prepared material contains rhomb-centered hexagonal $MgCO_3$ and carbon (see curve 1 in Fig 2a). The removal of $MgCO_3$ by acid treatment is verified from the XRD pattern of the HCl treated sample with the complete disappearance of the diffraction peaks related to

$MgCO_3$. Comparative XRD patterns of CMFs ans ACMFs are shown in Fig. 2b. Only two broad diffraction peaks at 25.9° and 43.0° are observed, corresponding to (002) and (101) facets of the hexagonal graphite (JCPDS, No. 75-1621). After activation, (002) peak of ACMFs becomes the sharper to reveal higher graphitized degree than that of CMFs. The similar phenomenon had been observed from our previous reports [17].

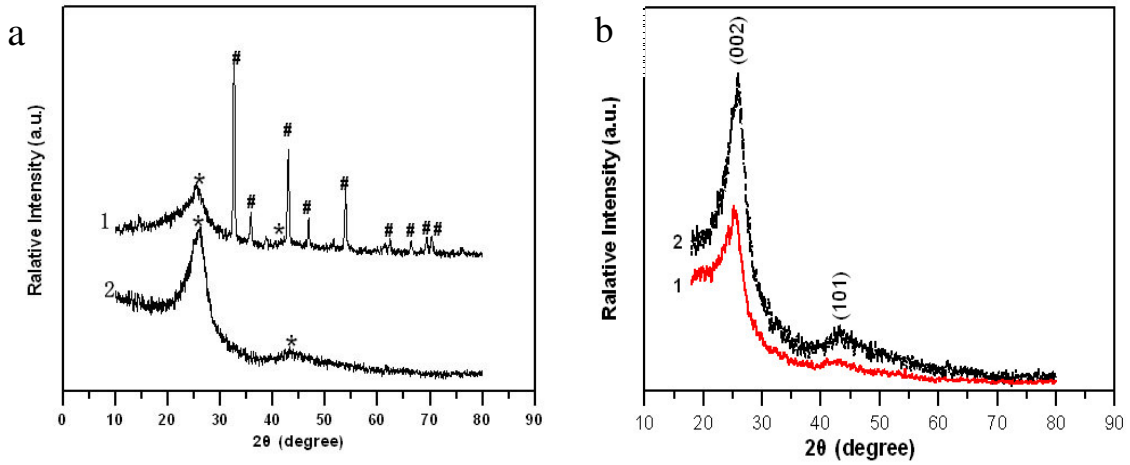

Figure 2. (a) XRD patterns of product treated before (1) and after (2) hydrochloric acid. (b) XRD patterns of CMFs (1) and ACMFs (2). #: $MgCO_3$; *: Carbon.

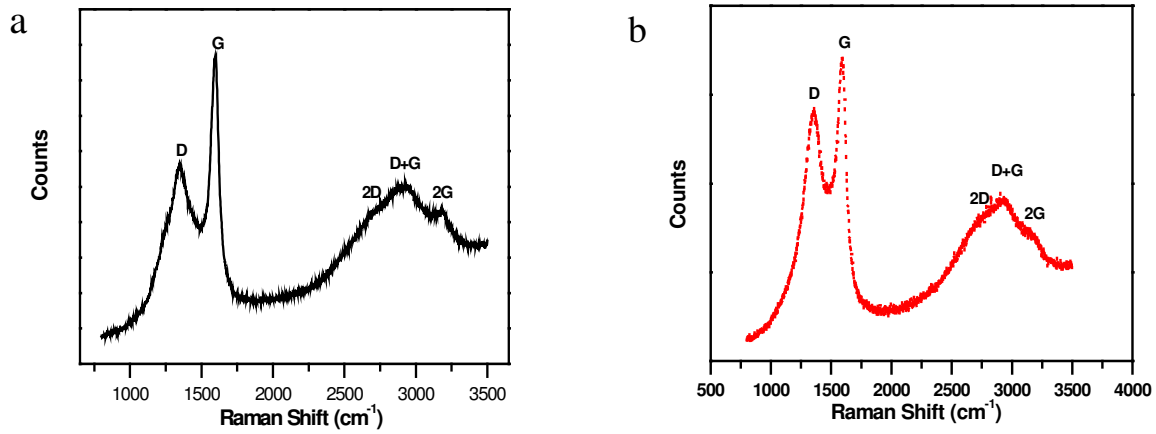

Figure 3. Raman spectra of CMFs (a) and ACMFs (b).

To further characterize the structure of CMFs and ACMFs, the Raman spectroscopy is used to measure carbon atom vibrations in as-synthesized carbon materials and provide further information about the crystallography for carbon materials. Fig. 3 shows the Raman spectra for CMFs ans ACMFs.

Two strong peaks at 1355.8 and 1595.9 cm^{-1} and three weak peaks at 2710, 2935 and 3177 cm^{-1} are observed. The sharp peak at 1595.9 cm^{-1} is attributed to the vibration of sp^2-bonded carbon atoms and is named the first-order G-band. The peak at 1355.8 cm^{-1} is assigned to the vibration of the D-band carbon atoms with dangling bonds in plane terminations of the disordered structure. The illegible peak at 2710 cm^{-1} is an overtone of the disordered carbon (2D-band) prepared at low temperature. Other weak peaks at 2935 and 3177 cm^{-1} are assigned to the combination of the hexagonal graphite and disordered mode (D+G) and the second-order G peak (2G). Generally, the intensity (*I*) ratio of the D and G bands is applied to evaluate the defect in carbon materials. That is, the larger the intensity ratio and the more the defects. D band of ACMFs after activation has been visibly intensified, which I_D / I_G ratio of D and G bands is 0.87. However, that of CMFs is 0.68 only. The increase of the defect indicates that some hydrophilic functional groups are formed at the surface of ACMFs via the activation. It is very important for carbon materials to be applied for EDLCs.

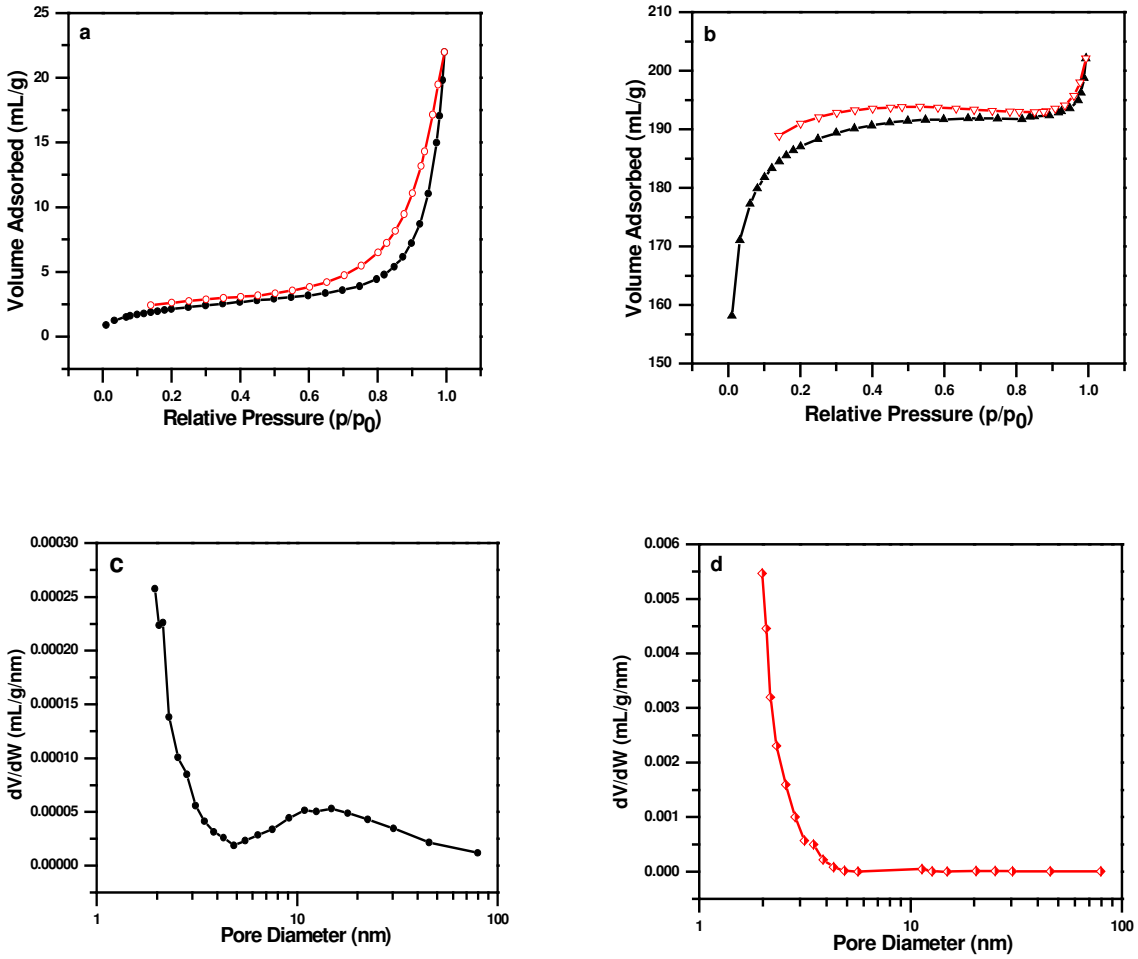

Figure 4. Nitrogen adsorption-desorption isotherms of CMFs (a) and ACMFs (b) and pore size distribution of CMFs (c) and ACMFs (d).

Nitrogen adsorption-desorption method is employed to measure the surface properties of CMFs and ACMFs at 77 K. The N_2 adsorption-desorption isotherms and pore size distribution of CMFs and ACMFs are shown in Fig. 4. The isotherm for CMFs (Fig. 4a) is the type □according to the International Union of Pure and Applied Chemistry (IUPAC) classification, as reported by Rodriguez [18]. The curve presents a increase slowly from P/P_o = 0.1 to 0.8 owing to capillary suction at the site of the mesopores and a sharp increase in P/P_o ranging from 0.9 to 0.99 due to strong capillary condensation. The results illustrate that pore structure of CMFs is mesopore and exists in irregular pore size distribution, as supported by its pore size distribution curve in Fig. 4c where both 2.1 nm and 15 nm peaks are displayed and small BET surface area (8.07 m^2 g^{-1}) is obtained. However, after activated treatment, the isotherm of ACMFs (see Fig. 4b) is typical and the sharp increase in curve from P/P_o = 0 to 0.1 is attributed to rapid adsorption in the micropores. A narrow pore size distribution centered at 1.94 nm is shown in Fig. 4d. To compare with y-axis of Fig. 4a, N_2 adsorption capacitance increases much bigger in Fig. 4b. These results clarify that the specific surface area with the activation is significantly increased and the maximum is 632 m^2 g^{-1} and is seventy times more than that of CMFs.

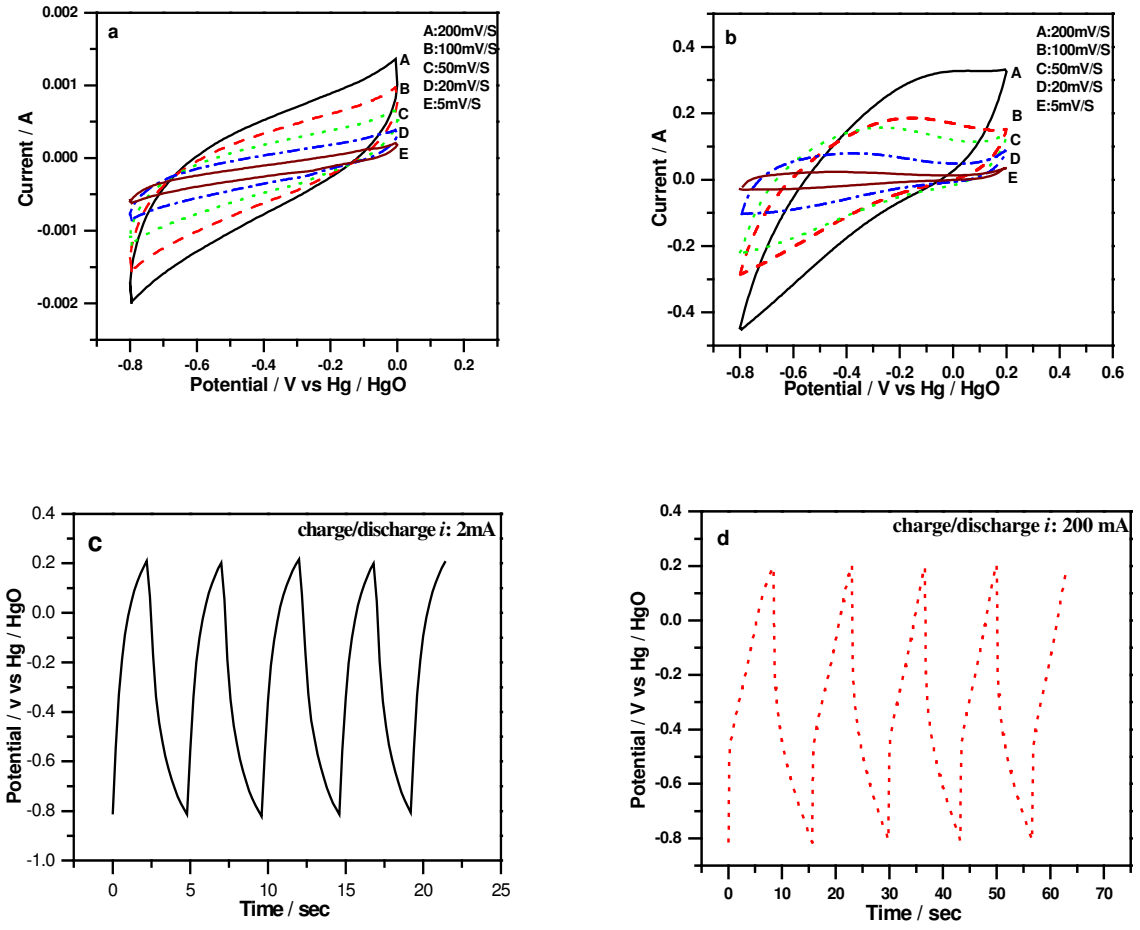

Figure 5. Cyclic voltammograms for CMFs (a) and ACMFs (b) and galvanostatic charge/discharge curves of CMFs (c) and ACMFs (d). The loading of CMFs: 27.5mg and that of ACMFs: 18 mg.

Owing to ACMFs with higher BET surface area and suitable pore structure, ACMFs are applied for EDLCs. A cyclic voltammetry is especially valuable and is the preferred method for studying double-layer capacitor materials and resulting electrochemical capacitor (EC) devices since it provides detailed information directly on the double-layer capacitance [19]. Fig. 5a and b show the comparison for the capability of CMFs and ACMFs via their cyclic voltammograms (CVs). Obviously, the capacitance of ACMFs is larger than that of CMFs.

An ideal double layer capacitance behavior of a carbon material electrode is expressed in the form of a rectangular shape on the voltammetry characteristics. However, the slopes of current variation vs potentials are obvious (see Fig. 5a) and indicate that forms IR drops in the carbon material electrodes. IR drops could be caused by two reasons involving no additional conductive reagent such as carbon black and the resistance of PTFE. Compared Fig. 5b to Fig .5a, under the low scan rate, CVs for ACMFs are not tilted to illustrate the unrestricted motion of electrolytes in the pores at this slow double-layer formation situation and also the conductivity of ACMFs is superior to that of CMFs. With the increase of scan rate, the CVs become tilted. This reflects that at high scan rates the IR drop for electrolyte motion in carbon pores affects the double layer formation mechanism, in which the charge stored is recognized to be distributed [20, 21]. The increase in the cathodic and anodic current with the scan rate intensifies the potential difference between the top and bottom of the pores and thus results in the delayed current response as shown in the tilted voltammograms [22].

The specific capacitance (C) of electrodes is calculated according to the following Eq (1) from charge/discharge measurement of CVs:

$$C = \frac{Q}{WV} = \frac{\int idt}{W\Delta V} \qquad (1)$$

where i, W and ΔV are the sample current and the weight of active materials and the total potential deviation of the voltage window, respectively. The compared data calculated from CVs of CMFs and ACMFs is listed in Table 1. The calculated results reveal that C of ACMFs is much larger than that of CMFs. With increasing scan rate, the specific capacitance is visibly decreased. The maximum specific capacitance for single electrode is 167.1 F g^{-1} obtained from CVs of ACMFs under low scan rate of 5 mV s^{-1}. Simultaneously, area-normalized C and energy density (E_D) of CMFs and ACMFs are also summarized in Table 1. The highest E_D for ACMFs is 83.6 kJ kg^{-1} at scan rate of 5 mV s^{-1}.

A complementary procedure of recording charge/discharge relations at constant-currents is usually employed for testing the practical capacitance of carbon materials. The charge/discharge behaviours of CMFs and ACMFs are investigated, as shown in Fig. 5c and d. These curves exhibit the relationships of the potential V vs time t is non-linearity in part. The similar phenomenon was found when Subramanian et al. investigated the electrochemical characterizations of single-walled carbon nanotube composites as electrode materials in supercapacitor [23]. Conway's group gave three factors to explain this involving (1) that of the direct ESR; (2) and of redistribution of charge within the pores of the carbon material structure during charging or discharging; (3) any pseudocapacitance contribution due to redox-active surface functional groups [19]. The specific capacitance (C) for materials from charge/discharge curves is denoted as:

$$C = \frac{it}{W\Delta V} \qquad (2)$$

where i, t, W and ΔV are the constant current and charge time and the weight of active materials and the total potential deviation, respectively. The gravimetric C calculated from charge/discharge curves for CMFs and ACMFs is 0.32 F g^{-1} and 186.5 F g^{-1}, respectively. A maximum area-normalized C is 30μF cm^{-2}. Visibly, the capability for charge storage in ACMFs is significantly improved. Power density of ACMFs is 11.1 kW kg^{-1} calculated from 11 A g^{-1} charge/discharge curve. Galvanostatic charge/discharge experiments verify that ACMFs can undergo quick charge/discharge at the large current density of 11 A g^{-1}. ACMFs could be the potential electrode materials for the application in supercapacitor.

Table 1. The specific capacitances(C) and energy density(E_D^*) calculated from CVs at the CMFs and ACMFs electrodes for aqueous electrolyte 6 mol L^{-1} KOH

Electrode		5 mV s^{-1}	20 mV s^{-1}	50 mV s^{-1}	100 mV s^{-1}	200 mV s^{-1}
CMFs	Gravimetric C (F g^{-1})	1.04	0.63	0.43	0.31	0.21
	Area-normalized C (μF cm^{-2})	13	7.9	5.4	3.9	2.6
	E_D (kJ kg^{-1})	0.33	0.20	0.14	0.10	0.07
ACMFs	Gravimetric C (F g^{-1})	167.1	132.6	98.3	50.9	37.0
	Area-normalized C (μF cm^{-2})	26.4	21.0	15.6	8.0	5.8
	E_D (kJ kg^{-1})	83.6	66.3	49.2	25.5	18.5

* $E_D = 0.5\ C\ V^2$

4. CONCLUSIONS

One-step pyrolysis method has been employed to directly synthesize the carbon microflakes. The activated carbon microflakes possess higher graphitized degree and larger specific surface area and the specific capacitance has been significantly improved. the results of cyclic voltammetry indicate high energy density (83.6 kJ kg^{-1}) for ACMFs at low scan rate of 5 mV s^{-1} and galvanostatic charge/discharge experiments illustrate that ACMFs can undergo large-current quick charge/discharge and high power density (11.1 kW kg^{-1}) is obtained at 11 A g^{-1}. ACMFs could be the potential electrode materials for the application in EDLCs.

ACKNOWLEDGMENTS

The authors wish to acknowledge financial support from the Natural Science Foundation of China (20876067) and the Union Foundation of NSFC and Guangdong Province (U0734005) and the Young-teacher Fund of Jinan University (51208023).

References

1. P.M. Ajayan, J.M. Nugent, R.W. Siegel, B. Wei and Ph. Kohler-Redlich, *Nature* 404(2000)243
2. S. Álvarez, T. Valdés-Solís and A.B. Fuertes, *Mater. Res. Bull.,* 43 (2008) 1898
3. C.M. Yang, Y.J. Kim, M, Endo, H. Kanoh, M. Yudasaka, S. Iijima and K. Kaneko, *J. Am. Chem. Soc.,* 129(2007)20
4. D.S. Yuan, C.W. Xu, Y.L. Liu, S.Z. Tan, X. Wang, Z.D. Wei and P.K. Shen, *Electrochem. Commun.,* 9((2007))2473
5. C.W. Xu, Y.L. Liu and D.S. Yuan, *Int. J. Electrochem. Sci.,* 2(2007)674
6. T.W. Ebbesen and P.M. Ajayan, *Nature,* 358(1992) 220
7. Y.H. Wu and B.J.Yang, *Nano Lett.,* 2(2002)355
8. Y. H. Wu, B. J. Yang, G. C. Han, B. Y. Zong, H. Q. Ni, P. Luo, T. C. Chong, T. S. Low and Z. X. Shen, *Adv. Funct. Mater.,* 12(2002)489
9. C.C. Chen, C.F. Chen, I.H. Lee and C.L. Lin, *Diam. Relat. Mater.,* 14(2005)1897
10. J.B. Yang, L.C. Ling, L. Liu, F.Y. Kang, Z.H. Huang and H. Wu, *Carbon,* 40(2002)911
11. Q. Cai, Z.H. Huang, F.Y. Kang and J.B. Yang, *Carbon,* 42(2004) 775
12. A.B. Fuertes and I. Menendez, *Sep. Purif. Technol.,* 28(2002) 29
13. W.L. Zhou, M. Yoshino, H. Kita and K. Okamoto, *J. Membrane Sci.,* 217(2003)55
14. T.A. Centeno, J.L. Vilas and A.B. Fuertes, *J. Membrane Sci.,* 228(2004)45
15. K.Z. Li, J. Wei, H.J. Li, Y.L. Zhang, C. Wang and D.S. Hou, *Appl. Surf. Sci.,* 253(2007)7365
16. D.S. Yuan, Y.L. Liu, Y. Xiao and L.Q. Chen, *Mater. Chem. Phys.,* 112(2008)27
17. D.S. Yuan, J.X. Chen, J.H. Zeng and S.X. Tan, *Electrochem. Commun.,* 10(2008)1067
18. N.M. Rodriguez, *J. Mater. Res.,* 8(1993)3233
19. J.J. Niu, W.G. Pell and B.E. Conway, *J. Power Sources,* 156(2006)725
20. B.E. Conway, Electrochemical Supercapacitors Scientific Fundamentals and Technological Application, Kluwer/Plenum, New York, (1999)
21. L.G. Austin and E.G. Gagnon, *J. Electrochem. Soc.*, 120(1973)251
22. H.Y. Liu, K.P. Wang and H.S. Teng, *Carbon,* 43 (2005) 559
23. V. Subramanian, H.W. Zhu and B.Q. Wei, *Electrochem. Commun.,* 8 (2006) 827